

---

# Hyperspectral Imaging to Classify Counterfeit Risk in Pharmaceuticals

---

Kenan Erol<sup>1</sup> Jolene Bressi<sup>2</sup> Alex Wong<sup>1</sup>

## Abstract

Counterfeit pharmaceuticals pose a significant global health risk. These counterfeit drugs are visually indistinguishable from their real counterparts. These similarities lead people to mistakenly take ineffective or even harmful active pharmaceutical ingredients (API), potentially causing serious adverse health effects or death.

This work explores the potential of hyperspectral imaging (HSI), which captures detailed spectral information beyond human vision, combined with deep learning for non destructive pill analysis. HSI provides a unique spectral analysis for materials by measuring reflectance across hundreds of narrow wavelength bands. We developed a pipeline to put such HSI data through preprocessing, segmentation using Segment Anything Model 2 (SAM2), spectral patch extraction, and training of adapted Convolutional Neural Networks (CNNs).

We address two key tasks: multi-class classification of six different drug types, and binary classification distinguishing authentic spectral patches from synthetically generated “fake” patches designed to simulate the spectral differences one might expect. We used datasets acquired by a Lumo spectral imager scanning trays containing 100 pills, producing 256 bands. The drug classes used were bromazepam, ecstasy (MDMA), clonazepam, oxycodone, tramadol, and zopiclone. Our adapted ResNet-18 model achieves 100% accuracy on the drug classification task. The model achieves 98.77% accuracy on the real vs fake task when using augmentations targeted at specific bands. Augmentations to bands 0-130 and

81-130 were tried with results becoming more effective based on the strength of the augmentations. These results demonstrate the promise of HSI and deep learning for pharmaceutical analysis, while highlighting the need for further validation with physically acquired counterfeit samples.

## 1. Introduction

Counterfeit pharmaceutical represent a critical threat to public health worldwide, contributing to treatment failure and increased mortality ([WorldHealthOrganization](#)). A major challenge lies in the fact that counterfeit pills are often designed to be visually indistinguishable from their genuine counterparts, rendering simple visual inspection unreliable. Traditional methods for verifying authenticity, such as laboratory-based chemical analysis are accurate and reliable, but are too time-consuming, expensive, and unsuitable for point-of-care level of screening ([Alsallal et al., 2018](#)).

Hyperspectral imaging (HSI) offers a promising alternative for non-destructive material analysis. By capturing image data across hundreds of narrow, contiguous spectral bands (typically spanning visible and near-infrared ranges), HSI acquires a unique spectral signature for each pixel, reflecting the material’s chemical composition and physical structure ([ElMasry & Sun, 2010](#)). This rich spectral information, invisible to the human eye or standard RGB cameras, holds the potential to differentiate between substances with subtle chemical variations, such as those found between genuine and counterfeit drugs ([Wilczyński et al., 2016](#)).

Deep learning, particularly Convolutional Neural Networks (CNNs), has revolutionized image analysis tasks. Adapting CNNs to handle the high dimensionality of HSI data allows for the automatic extraction of discriminative spatio-spectral features.

This project investigates the feasibility of combining HSI and adapted CNNs for two primary tasks in pharmaceutical analysis:

**Multi-class Drug Identification:** Accurately classifying different types of pills based on their spectral signatures.

**Real-vs-Fake Classification:** Distinguishing between spec-

---

<sup>1</sup>Department of Computer Science, Yale University, New Haven, CT <sup>2</sup>School of Public Health, Yale University, New Haven, CT. Correspondence to: Kenan Erol <[kenan.erol@yale.edu](mailto:kenan.erol@yale.edu)>, Jolene Bressi <[jolene.bressi@yale.edu](mailto:jolene.bressi@yale.edu)>, Alex Wong <[alex.wong@yale.edu](mailto:alex.wong@yale.edu)>.

Submitted to the Department of Computer Science at Yale University for CPSC 290 - Directed Research.

tral data from authentic pills and synthetically altered data designed to mimic potential counterfeit anomalies.

To achieve this, we developed a pipeline converting HSI data in numpy arrays, segmenting pills using the Segment Anything Model 2 (SAM 2) (Ravi et al., 2024), extracting representative spectral patches, generating of synthetic "fake" data via targeted spectral augmentation, and training and evaluating adapted ResNet-18 models. Our results demonstrate high classification accuracy for both tasks on the available dataset, suggesting the potential of this approach. However, we emphasize the synthetic nature of the "fake" data and the need for validation against real-world counterfeit samples.

This report details our methodology (Section 3), presents the experimental results (Section 4), discusses their implications and limitations (Section 5), and concludes with future directions (Section 6).

## 2. Background

### 2.1. The Counterfeit Drug Problem

The production and trafficking of counterfeit and substandard medicines is a growing global crisis, affecting both developing and developed nations. The World Health Organization estimates that a significant percentage of drugs in circulation in some regions may be counterfeit, ranging from ineffective placebo formulations to those containing incorrect ingredients, incorrect dosages, or even toxic substances (WorldHealthOrganization). Opioid-containing medications are a particular concern due to the ongoing overdose epidemic (Tanz et al., 2022). The difficulty in visually distinguishing fakes creates the need for advanced analytical techniques.

### 2.2. Existing Detection Methods and Limitations

Current methods for drug verification span a spectrum of complexity and accessibility. Visual inspection is the simplest but least reliable method. Laboratory techniques like High-Performance Liquid Chromatography (HPLC) and Mass Spectrometry (MS) provide definitive chemical analysis but are destructive, slow, costly, and require laboratory infrastructure (Rao et al., 2023). Techniques like X-ray Fluorescence (XRF) have been explored (Alsallal et al., 2018) but require specialized, bulky equipment. There is a clear need for rapid, reliable, non-destructive, and portable methods for drug screening.

### 2.3. Hyperspectral Imaging (HSI)

Unlike standard cameras capturing broad Red, Green, and Blue bands, HSI systems acquire data cubes containing spatial information (x, y dimensions) and spectral information

( $\lambda$  dimension) across numerous narrow wavelength bands (ElMasry & Sun, 2010). Each pixel in the HSI cube contains a spectrum representing the light interaction (reflectance, absorbance, or fluorescence) with the material at that location. This spectral signature is highly sensitive to the chemical and physical properties of the substance, enabling the differentiation of materials that appear identical visually. The potential of HSI for pharmaceutical analysis, particularly for detecting subtle variations indicative of counterfeiting, has been demonstrated (Wilczyński et al., 2016). While specialized HSI cameras exist, research also explores reconstructing hyperspectral information from more accessible sensors, potentially including smartphones under specific conditions (He et al., 2023) (Stuart et al., 2021), although this work utilizes data from a dedicated HSI camera.

### 2.4. Deep Learning for Hyperspectral Image Analysis

Applying deep learning, especially CNNs, to HSI data presents unique challenges and opportunities. Common strategies include:

Band Selection/Reduction: Using techniques like Principal Component Analysis (PCA) or selecting specific informative bands before feeding data to a standard 2D CNN.

Adapted 2D CNNs: Modifying the first convolutional layer of standard 2D CNN architectures (like ResNet (He et al., 2016), VGG to accept the high number of spectral channels as input channels. This approach leverages powerful pre-trained architectures while accommodating the spectral dimension.

3D CNNs: Employing convolutions in both spatial (x, y) and spectral ( $\lambda$ ) dimensions to explicitly learn spatio-spectral features. These models can be more complex and data-hungry.

This project focuses on adapting standard 2D CNNs (ResNet-18) due to their proven effectiveness and the availability of established architectures.

## 3. Methodology

Our methodology involves several stages, from raw data processing to model training and evaluation, implemented using Python, PyTorch, and libraries like NumPy, scikit-learn, and Matplotlib.

### 3.1. Dataset

The primary dataset consists of hyperspectral images of pharmaceutical pills provided by collaborators at the Swedish National Forensic Centre and Yale School of Public Health. The data includes samples from six distinct drug classes: Bromazolam, Clonazepam, Ecstasy (MDMA), Oxycodone, Tramadol, and Zopiclone. The raw data was

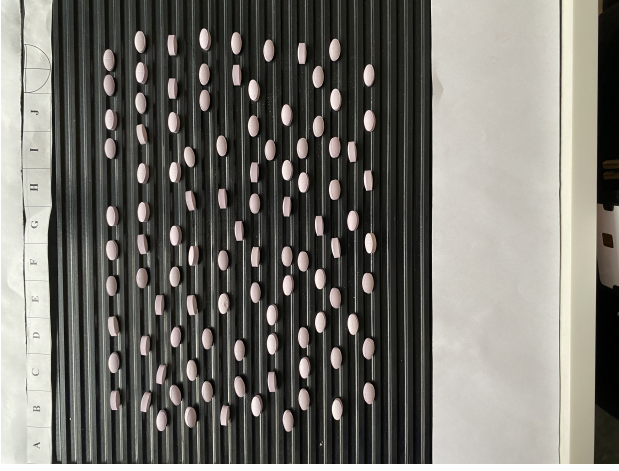


Figure 1. Picture of the tray taken with an iPhone.

captured using an HSI camera system by LUMO, resulting in ENVI format files (.raw data cubes and .hdr header files). Each hyperspectral cube has spatial dimensions of 400x320 pixels and 256 spectral bands, covering a Wavelength Range from approximately 936 nm to 2541 nm. Example visualizations of the pre and post HSI images of the drug trays can be seen in Figure 1.

### 3.2. Preprocessing and Patch Extraction

#### 3.2.1. DATA CONVERSION

Raw ENVI files were converted to NumPy arrays (.npy) using a custom script (tools/convert\_data.py) leveraging the spectral library, preserving the original data structure.

#### 3.2.2. PILL SEGMENTATION

We employed the Segment Anything Model 2 (SAM 2) (Ravi et al., 2024), specifically the sam2.1\_hiera\_base\_plus.pt checkpoint, for automatic pill segmentation. The preproc\_patch.py script processes each .npy image: An RGB-like representation (mean across spectral bands, normalized) is generated as input for SAM 2. SAM2AutomaticMaskGenerator generates multiple mask proposals for each image. Masks are filtered based on predicted IoU score ( $\geq \text{MIN\_IOU\_SCORE}$ , e.g., 0.5) and area (between MIN\_PILL\_AREA and MAX\_PILL\_AREA, e.g., 50-170 pixels) to isolate probable pill masks (see Figure 2).

#### 3.2.3. PATCH EXTRACTION

For each valid pill mask: A bounding box is computed. The bounding box is adjusted to be square, slightly enlarged (10%), and clipped to image boundaries. The hyperspec-

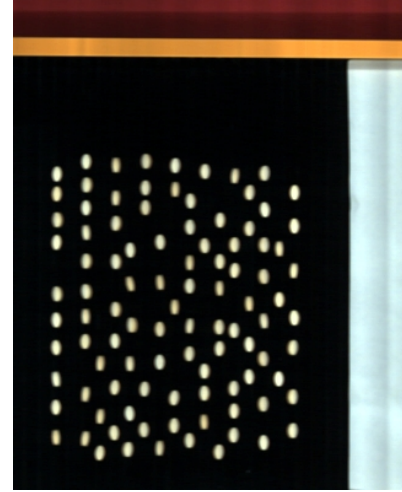


Figure 2. RGB representation of the HSI tray generated by the LUMO Scanner.

tral data within the final bounding box is extracted. The extracted patch is resized to a fixed size (224x224 pixels) using bilinear interpolation (resize\_patch function).

### 3.3. Synthetic "Fake" Data Generation

Due to the unavailability of physical counterfeit samples, we generated synthetic "fake" data to train the real-vs-fake classifier.

**Source Selection:** We performed random sampling on the real patches generated in the previous step, selecting 50% of patches from each drug class (totaling around 5000 patches) using augment\_patches.py.

**Augmentation:** The selected real patches were augmented using augment\_patches.py to create corresponding "fake" versions. Specific bands were augmented: either bands 0-130 (corresponding to wavelength range 936.66-1764.99nm) or 81-130 (range 1449.79-1764.99nm). The vicinity of these bands have been shown to show spectral differences for drugs like MDMA and Viagra (Marmion & Wilczynski (Wilczyński et al., 2016)). There were three versions of these fake versions: weaker augmentations on wavelength range 1449.79-1764.99 nm, stronger augmentations on the same wavelength range, and the same strong augmentations on the range 936.66-1764.99 nm. The augmentations of Gaussian noise, intensity scaling, and intensity offset were applied sequentially in the following way:

**Gaussian Noise:** Additive noise with mean 0.0 for weak and strong, standard deviation 0.05 for weak and 0.25 for strong.

**Intensity Scaling:** Multiplicative scaling with a factor randomly chosen between 0.9 and 1.1 for weak, 0.7 and 1.3 for strong.

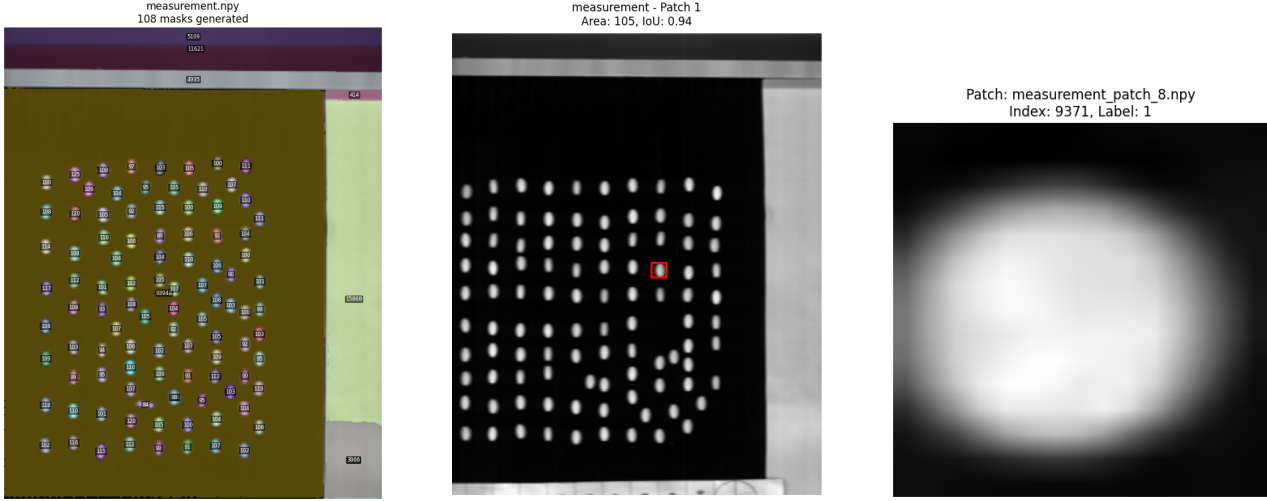
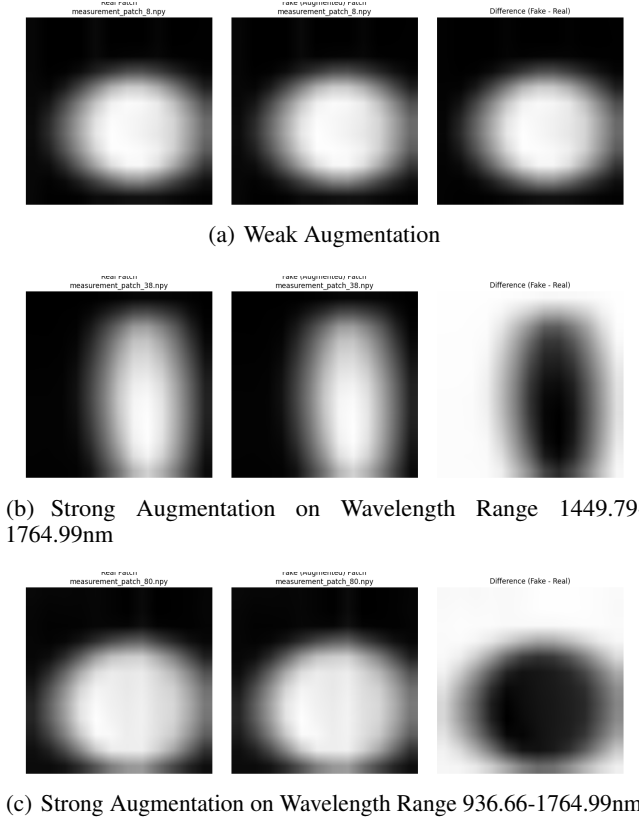


Figure 3. Generation of masks, capture of pills, and visualization of resulting patch.



(c) Strong Augmentation on Wavelength Range 936.66-1764.99nm

Figure 4. Visualizations of given real patches and their corresponding fake patches, based on the strength of the augmentation.

**Intensity Offset:** Additive offset randomly chosen between -0.05 and 0.05 for weak, -0.2 and 0.2 for strong augmentations.

Figures 3 and 4 visualize how these augmentations changed the patch profiles.

### 3.4. Dataset Splitting

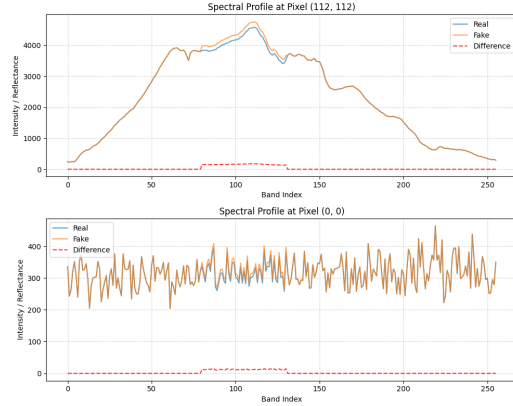
Distinct splitting strategies were used for the two tasks:

**Drug Classification:** The patch dataset was split into training (80%) and testing (20%) sets using sklearn's train test split function.

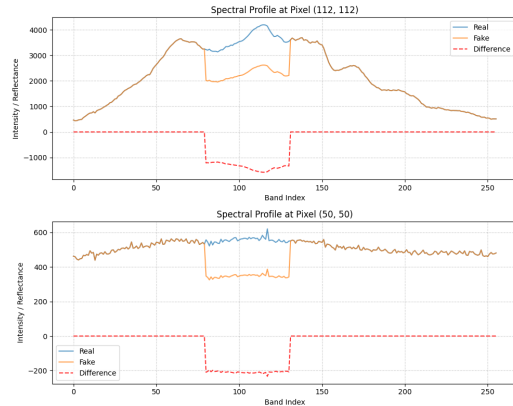
**Real vs. Fake Classification:** A specific strategy was employed to handle the paired nature of the data and storage limitations (10000 real patches total, 5000 used to generate 5000 fakes): The 5000 real patches used as sources for the fake data and their corresponding 5000 fake patches were treated as pairs. These 5000 pairs were split 80/20, resulting in 4000 pairs (4000 real + 4000 counterfeit) for training and 1000 pairs (1000 real + 1000 counterfeit) for testing. This ensures the model sees corresponding real/fake examples during training and testing. The remaining 5000 real patches (not used for augmentation) were separately split 80/20, yielding 4000 for training and 1000 for testing. The final training set comprised 12,000 patches. The final test set comprised 3,000 patches.

### 3.5. Model Architecture

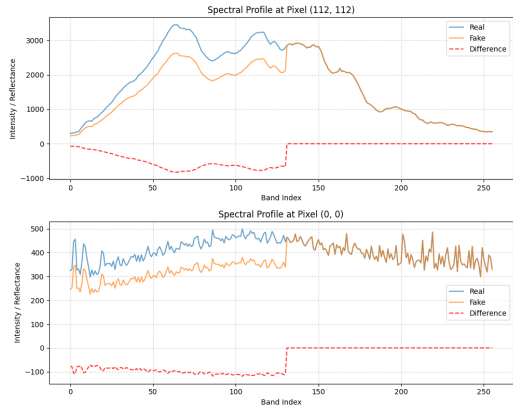
We adapted the ResNet-18 standard CNN architecture (He et al., 2016). The primary modification involved changing the first convolutional layer (conv1 in ResNet) to accept the number of hyperspectral bands (256) as input channels instead of the standard 3 (RGB). The final fully connected layer (classifier) was replaced with a new layer outputting logits for the required number of classes (6 for drug classifi-



(a) Weak Augmentation on Wavelength Range 1449.79-1764.99nm Spectral Profile



(b) Strong Augmentation on Wavelength Range 1449.79-1764.99nm Spectral Profile



(c) Strong Augmentation on Wavelength Range 936.66-1764.99nm Spectral Profile

*Figure 5.* The spectral profiles of the real and fake patches, graphing band indices vs intensity.

cation, 2 for real/fake classification).

### 3.6. Training

Models were trained using the `train_classification_hyper.py` script. The patches went under random transforms like random flips and random intensity scaling.

Optimizer: Stochastic Gradient Descent (SGD) was used.

Loss Function: Cross-Entropy Loss was used.

Learning Rate: An initial learning rate was set (e.g., 0.005 for ResNet-RF, 0.001 for ResNet Drug ID) with scheduled decay.

Epochs: Trained for a fixed number of epochs (e.g., 30-50).

Hardware: Training was performed on NVIDIA GPUs from the Grace cluster using CUDA.

### 3.7. Evaluation

Model performance was evaluated on the held-out test sets using `run_classification_hyper.py`. The primary metric was accuracy. We also computed and analyzed:

Classification Report: Precision, Recall, and F1-score per class.

Confusion Matrix: To visualize misclassifications between classes (See Figure 5).

## 4. Results

We evaluated the performance of the adapted ResNet-18 models on the test sets defined by our splitting strategies.

### 4.1. Drug Classification

The ResNet-18 model trained for multi-class drug identification achieved 100% accuracy on the test set (2000 patches derived from unseen source images). The confusion matrix (Figure 6a) showed a perfect diagonal, indicating no misclassifications between the six drug types in the test set.

### 4.2. Real vs. Fake Classification

The ResNet-18 model trained to distinguish between real patches and their synthetically augmented counterparts (using noise, scaling, and offset) achieved accuracies of 67%, 98.07%, 98.73% for the weak, strong on bands 81-130, and strong on bands 0-130 augmented patches, respectively. Notably, the weakly augmented fakes were indistinguishable to the model, as it guessed all of them to be real drugs (Figure 6b). The stronger augmentations performed well in both cases (Figures 6c and 6d).

These results indicate that the adapted CNN models were highly effective in learning discriminative spectral features for both identifying different drug types and detecting the

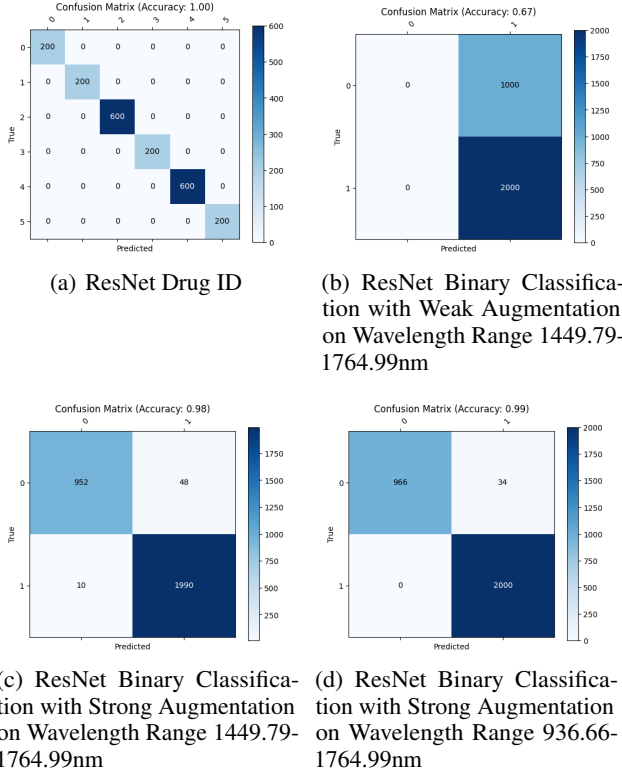


Figure 6. The confusion matrices of the different models and configurations of models.

specific synthetic alterations introduced in the targeted spectral bands.

## 5. Discussion

The experimental results demonstrate the strong potential of combining hyperspectral imaging with adapted deep learning models for pharmaceutical analysis.

The 100% accuracy achieved in the multi-class drug identification task suggests that the six drug types included in our dataset possess distinct spectral signatures within the captured wavelength range (936-2541 nm) that are learnable by a ResNet-18 architecture. This confirms the premise that HSI can capture chemically relevant information for differentiating pharmaceuticals non-destructively.

The 98% accuracy obtained for the real-vs-fake classification task is also promising. It indicates that the model is sensitive to the specific augmentations (noise, scaling, offset) applied within the targeted spectral bands, which could be relevant for identifying certain types of anomalies or deviations from a standard spectral profile of a genuine pharmaceutical.

## 5.1. Limitations

It is crucial to interpret these results within the context of the study's limitations.

**Synthetic Fakes:** The most significant limitation is the use of synthetically generated "fake" data. We were originally going to train with actual counterfeit samples, but we were unable to acquire these in time for the study. The augmentations applied, while designed to introduce spectral variations, may not accurately represent the complex chemical and physical differences found in real-world counterfeit or substandard drugs. Real counterfeits might involve different active ingredients, binders, coatings, or manufacturing processes, leading to spectral differences potentially unlike those simulated by our augmentations. Therefore, the 98% accuracy reflects the model's ability to detect our specific augmentations and cannot be directly extrapolated to performance on actual counterfeits.

**Controlled Conditions:** The HSI data was acquired under controlled laboratory conditions (lighting, camera setup). Real-world deployment, especially using potentially lower-fidelity or mobile HSI systems, would introduce significant variability (e.g., ambient light, distance, angle) that could degrade performance.

**Augmentation Strategy:** While the selection of the targeted bands was motivated by preliminary analysis, this range might not be universally optimal. The specific augmentation types and parameters were chosen heuristically and might not cover the full spectrum of potential counterfeit characteristics for all drugs.

**Future Work:** Addressing these limitations requires several avenues for future research. Validating the approach using a diverse set of physically acquired, chemically verified counterfeit and substandard drug samples is paramount. Further study is needed into the spectral characteristics of the group of drugs that our project covers as the bands with the highest significance might vary across different pharmaceuticals. Finally, assessing performance under more realistic acquisition conditions and exploring the feasibility of deployment on portable or smartphone-based HSI systems (Stuart et al., 2021) (He et al., 2023) are essential steps towards practical application.

## 6. Conclusion

This project successfully demonstrated the application of hyperspectral imaging and adapted deep learning models for pharmaceutical analysis. We developed a pipeline for processing HSI data, segmenting pills using SAM 2, extracting spectral patches, and training CNNs modified for high-dimensional input. Our models achieved excellent performance, with 100% accuracy in classifying six dif-

ferent drug types and 98% accuracy in distinguishing real spectral patches from synthetically augmented "fake" versions designed to simulate anomalies in specific spectral bands. These results highlight the potential of HSI as a non-destructive tool for capturing discriminative spectral fingerprints and the ability of deep learning models to learn these features effectively. However, the reliance on synthetic data for the real-vs-fake task necessitates caution. Future work must focus on validating these findings with authentic counterfeit samples and exploring robustness under real-world conditions (ie. with hyperspectral imaging done on a smartphone) before considering practical deployment.

## Acknowledgements

I would like to express my sincere gratitude to my advisor, Professor Alex Wong, for his guidance, support, and valuable insights throughout this project. I also thank Dr. Jolene Bressi and Ian Martin from the Yale School of Public Health and Professor Simon Dunne from the Swedish National Forensic Centre for providing the HSI dataset crucial for this work. I thank Professor Holly Rushmeier for her insights into using HSI data more effectively. This research utilized the Segment Anything Model 2 (SAM2) developed by Meta AI (Ravi et al., 2024). Computational resources were provided by the Yale Grace cluster. This project was undertaken as part of the CPSC 290 Directed Research course at Yale University under the supervision of the Director of Undergraduate Studies, Professor Theodore Kim.

## References

- Alsallal, M., Sharif, M. S., Al-Ghzawi, B., and Mlkat al Mutoki, S. M. A machine learning technique to detect counterfeit medicine based on x-ray fluorescence analyser. In *2018 International Conference on Computing, Electronics Communications Engineering (iCCECE)*, pp. 118–122, 2018.
- ElMasry, G. and Sun, D.-W. Chapter 1 - principles of hyperspectral imaging technology. In Sun, D.-W. (ed.), *Hyperspectral Imaging for Food Quality Analysis and Control*, pp. 3–43. Academic Press, San Diego, 2010. ISBN 978-0-12-374753-2. doi: <https://doi.org/10.1016/B978-0-12-374753-2.10001-2>. URL <https://www.sciencedirect.com/science/article/pii/B9780123747532100012>.
- He, K., Zhang, X., Ren, S., and Sun, J. Deep residual learning for image recognition. *2016 IEEE Conference on Computer Vision and Pattern Recognition (CVPR)*, Jun 2016. doi: 10.1109/cvpr.2016.90.
- He, Q., Li, W., Shi, Y., Yu, Y., Geng, W., Sun, Z., and Wang, R. K. Specamx: mobile app that turns unmodified smartphones into multispectral imagers. *Biomed. Opt. Express*, 14(9):4929–4946, Sep 2023. doi: 10.1364/BOE.497602. URL <https://opg.optica.org/boe/abstract.cfm?URI=boe-14-9-4929>.
- Marmion, M. and Wilczynski, S. Analysis and detection of drugs and counterfeit medicines with hyperspectral cameras. URL <https://proceedings.science/nir-abstracts/papers/analysis-and-detection-of-drugs-and-counterfeit-medicines-with-hyperspectral-cam?lang=en>.
- Rao, A. S., Dileep, B., and Madhusudhan, B. A review on "pharmaceutical analysis in the modern era: Advanced analytical methods". *IJNRD*, 2023. URL <https://www.ijnrd.org/papers/IJNRD2310099.pdf>.
- Ravi, N., Gabeur, V., Hu, Y.-T., Hu, R., Ryali, C., Ma, T., Khedr, H., Rädle, R., Rolland, C., Gustafson, L., Mintun, E., Pan, J., Alwala, K. V., Carion, N., Wu, C.-Y., Girshick, R., Dollár, P., and Feichtenhofer, C. Sam 2: Segment anything in images and videos. *arXiv preprint arXiv:2408.00714*, 2024. URL <https://arxiv.org/abs/2408.00714>.
- Stuart, M. B., McGonigle, A. J. S., Davies, M., Hobbs, M. J., Boone, N. A., Stanger, L. R., Zhu, C., Pering, T. D., and Willmott, J. R. Low-cost hyperspectral imaging with a smartphone. *Journal of Imaging*, 7(8), 2021. ISSN 2313-433X. doi: 10.3390/jimaging7080136. URL <https://www.mdpi.com/2313-433X/7/8/136>.
- Tanz, L. J., Dinwiddie, A. T., Mattson, C. L., O'Donnell, J., and Davis, N. L. Drug overdose deaths among persons aged 10–19 years — united states, july 2019–december 2021. *MMWR. Morbidity and Mortality Weekly Report*, 71(50):1576–1582, Dec 2022. doi: 10.15585/mmwr.mm7150a2.
- Wilczyński, S., Koprowski, R., Marmion, M., Duda, P., and Błońska-Fajrowska, B. The use of hyperspectral imaging in the vnir (400–1000 nm) and swir range (1000–2500 nm) for detecting counterfeit drugs with identical api composition. *Talanta*, 160:1–8, Nov 2016. doi: 10.1016/j.talanta.2016.06.057.
- WorldHealthOrganization. URL <https://www.who.int/news-room/fact-sheets/detail/substandard-and-falsified-medical-products>.